ISSN 1392–1320 MATERIALS SCIENCE (MEDŽIAGOTYRA). Vol. 21, No. 2. 2015

Humidity Sensing Elements Based on Zn-doped TiO_2 Films Prepared via a Sol-gel Method

Zvezditza NENOVA [1]*, Toshko NENOV [1], Stephan KOZHUKHAROV [2], Maria MACHKOVA [2]

[1] *Technical University of Gabrovo, 4 H.Dimitar Str., 5300 Gabrovo, Bulgaria*
[2] *University of Chemical Technology and Metallurgy, 8 Kliment Ohridski Blvd., 1756 Sofia, Bulgaria*

crossref http://dx.doi.org/10.5755/j01.mm.21.2.6244

Received 19 January 2014; accepted 02 June 2014

Humidity sensing elements have been prepared via a sol-gel method on the basis of titanium n-butoxide, doped with ZnO. By this method Zn-modified titania films have been deposited on alumina substrates with interdigitated silver palladium electrodes and subsequent sintering at temperatures of 400 °C and 800 °C. Scanning electron microscopy has been employed to determine the surface morphology of the films obtained. Structural and compositional characterizations have been done by X-ray diffraction analysis and energy dispersive X-ray spectroscopy. Electrical measurements of the characteristics and parameters of the obtained samples have been taken by an impedance analyzer within a frequency range from 100 Hz to 1 MHz. The impact of the Zn-dopant and sintering temperature on the samples' electrical properties has been studied. The samples obtained by the sol-gel method described can be used as humidity sensing elements which change their resistance given changes in relative humidity at frequencies of up to about 1kHz.
Keywords: humidity sensing elements, sol-gel method, titania, zinc dopant.

1. INTRODUCTION

Development of humidity sensors is of current interest since they are widely used in various fields. They are employed in humidity control of the environment and in many industrial processes such as chemical technologies, paper and textile industries, food processing, etc. These sensors play an important role in monitoring humidity in libraries, museums and galleries, the storage of food products at optimum conditions in warehouses. They are used in intelligent buildings to provide comfortable living conditions. In the field of medicine humidity sensors are incorporated into respiratory equipment, sterilizers, incubators and they are used in the manufacturing of pharmaceutical and biological products. In agriculture they are used to control humidity in greenhouses, soil, in storing of grain, etc. [1, 2].

Since the fields of application involve different operating conditions, the selection of materials for the sensing elements has to meet certain requirements to ensure normal operation of humidity sensors. They should have high sensitivity in the application range, fast response and small hysteresis.

Many materials have been investigated in view of their potential use as humidity sensing elements. These materials are based on polymers [3 – 6], ceramics [7 – 10] and composite materials [11 – 14]. Ceramic humidity sensors are to be preferred to the rest due to their thermal, physical and chemical stability [15]. They are developed on the basis of metal oxides as: Al_2O_3, SnO_2, TiO_2, Fe_2O_3, ZnO, ZrO_2, etc. [16]. Humidity sensing elements based on TiO_2 have been studied intensely because they have hydrophilic properties. They can be prepared as bulk ceramic elements, or as thick and thin films. The use of dopants improves the humidity sensing parameters based on TiO_2 [17 – 21]. Humidity sensing elements based on ZnO have also been studied [22 – 24]. The impact of different dopants on the characteristics and parameters of ZnO-based elements [8, 25 – 29], and the properties of ceramic and thick film humidity sensors based on ZnO-TiO_2 nanocomposites have also been investigated [30 – 33]. Compared to other frequently used dopants for metal oxide humidity sensors, the use of Zn as a dopant does not violate environmental regulations, which impose restrictions on the use of heavy metals [34, 35]. A sol-gel method has been increasingly applied to the preparation of thin film sensing elements. It allows a relatively easy preparation of these elements from various precursors.

This paper presents the results of studying humidity sensing elements based on Zn-doped TiO_2, and prepared by sol-gel method. Titanium n-butoxide (TBOT) was used as basic precursor, and ZnO served as a doping agent. The impact of the Zn-dopant and the sintering temperature on the humidity sensing properties of the obtained samples has been investigated.

2. EXPERIMENTAL PROCEDURE

2.1. Sample preparation

2.1.1. Preparation of the sol-gel system

Initially, 100 ml of TBOT, produced by Alfa Aesar – Karlsruhe (Germany), were mixed with 50 ml of n-butanol, (Fluka Switzerland) preliminarily heated up to 70 °C in a covered beaker, by dripping for 30 min, under stirring. Separately, about 1 g of ZnO was dissolved in 2 ml of concentrated hydrochloric acid to obtain a saturated solution of ZnO and was left for at least 30 min at ambient conditions. This solution was added to the main mixture, described above, and the resulting sol was left for 2 h at the same temperature. After cooling down to ambient temperature, the obtained sol-gel system was left for one week at 5 °C.

*Corresponding author. Tel. +359-66-854296; fax.: +359-66-801155.
E-mail address: *z_nenova@yahoo.com* (Z. Nenova)

2.1.2. Film deposition

Prior to depositing the film, alumina substrates with (10×18×0.5) mm size dimensions and interdigitated silver-palladium electrodes were immersed into pure acetone for one night, in order to remove all organic impurities from their surface. The film was deposited via dip-coating procedure by triple dipping into the solution for 30 min at 70 °C, and subsequent drying at the same temperature. Afterwards, the samples were sintered for 30 min, either at 400 °C, or at 800 °C. The respective sensor elements were denoted as S_400 and S_800 for the samples based on Zn-doped TiO_2 according their sintering temperature.

To evaluate the impact of the Zn-dopant on the properties of the corresponding humidity sensing elements, another set of samples was prepared by the same method without dopants. The latter served as reference samples for comparison. They are denoted as SRef_400 and SRef_800.

2.2. Measurements

To determine the properties of the surface films obtained, their distinctive features and the content of chemical elements, comparative observations by Scanning Electron Microscopy (SEM), together with Energy Dispersive X-ray Spectroscopy (EDX) were performed. SEM-images were taken by Scanning Electron Microscope TESCAN, SEM/FIB LYRA I XMU. The local compositions and map data analyses were studied by Energy Dispersion Spectrometer Quantax 200 of BRUKER detector.

Structural and compositional characterization was performed by X-ray diffractometry (XRD) on powder materials from the respective gels, sintered at 400 °C and 800 °C. The measurements were taken by Philips PW 1050, supported by CuKα - X-ray emitter. All the spectra were acquired in the angle range from $\theta = 10^o$ to $\theta = 100^o$, at scan rate $2\theta/\tau = 0.04^o$/s, and 1 s exposition per step.

The evaluation of the relation between the electrical parameters of the obtained samples and the relative humidity levels was performed with a calibration system VAPORTRON H-100BL, manufactured by Buck Research Instruments L.L.C., which is a high-performance, self standing temperature/humidity reference generator, and Precision Impedance Analyzer 6505P, product of Wayne Kerr Electronics Ltd. During the measurements, the respective samples were put inside the chamber of the calibration system at given temperature and relative humidity in the range of 15 % to 93 % with maximal deviation of up to ±1.5 %.

The resistance and capacitance of the samples were determined by the impedance analyzer for each humidity level, at frequencies ranging from 100 Hz to 1 MHz and 500 mV of the excitation signal. The results were used to obtain the respective samples characteristics.

3. RESULTS AND DISCUSSION

3.1. SEM, EDX and XRD analysis

SEM- and EDX-images of samples S_400 and S_800 are presented in Fig. 1. The SEM-images at lower magnification for both kinds of samples show that they consist of deposited aggregates on alumina substrates. Also, between these aggregates there are channel-shaped area with different length and width, providing larger contact surface for water vapors adsorption and subsequent condensation. On the other hand, the higher magnification SEM-images for the samples sintered at 800 °C reveal that the surface of the aggregates has a higher porosity, which is favorable for the adsorption of water molecules.

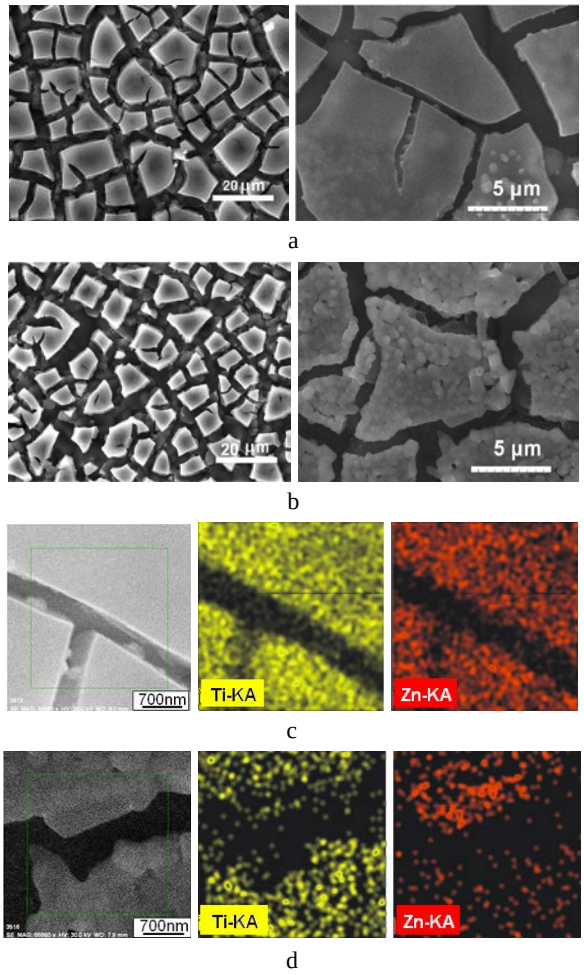

Fig. 1. SEM- and EDX-images: a and c – of S_400; b and d – of S_800, respectively

The selected high resolution EDX-images in Fig. 1, c and d, for the investigated samples confirm the presence of Ti and Zn in the surface deposits. In addition to the EDX analysis, carried out for element composition and distribution, structural XRD characterization was performed, as well. The aim was to clarify whether the surface deposits are composed of crystals of ZnO and TiO_2, or derivative zinc titanate is formed [36, 37].

Titanium dioxide exists in three main modifications: rutile, anatase, and brookite [38, 39]. At temperatures between 550 °C and about 1000 °C, anatase is irreversibly converted into the equilibrium rutile phase. The temperature of this transformation depends on the impurities or dopants present, as well as on the morphology of the sample [40].

Fig. 2 shows the XRD patterns obtained for powder materials of referent samples SRef_400 and SRef_800, sintered at 400 °C and 800 °C. The XRD analysis shows that the referent powder material sintered at 400 °C is composed of anatase phase (Fig. 2, a). At 800 °C, in this material phase transition of TiO_2 takes place – from anatase phase to rutile phase, which is confirmed by the results in Fig. 2, b.

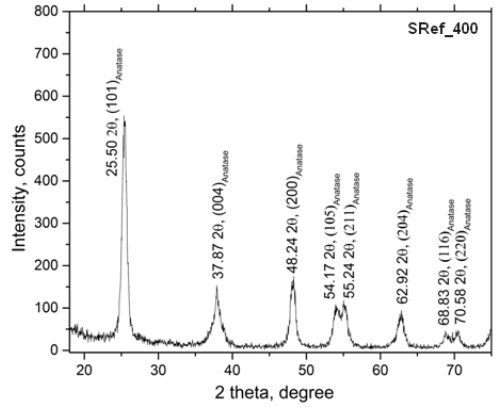

a

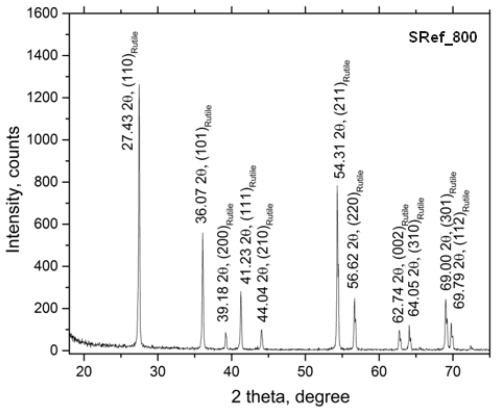

b

Fig. 2. XRD diagrams of powder materials of referent samples SRef_400 and SRef_800 sintered at: a – 400 °C; b – 800 °C

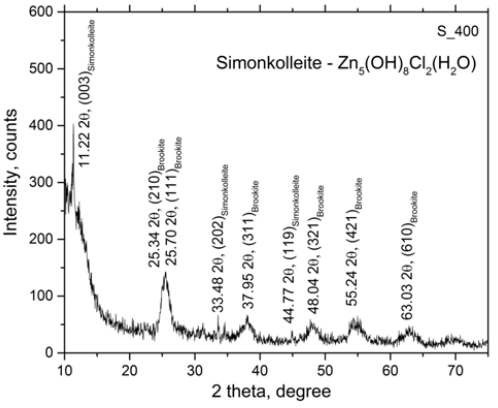

a

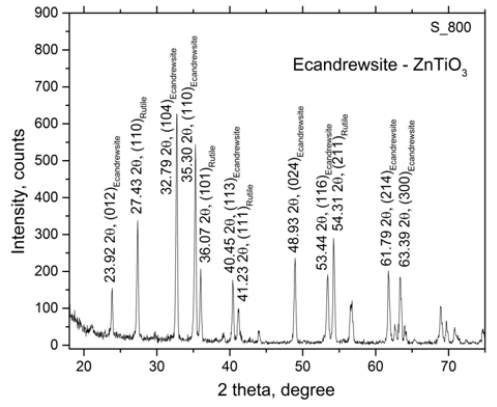

b

Fig. 3. XRD diagrams of powder materials of samples S_400 and S_800, doped with Zn and sintered at: a – 400 °C; b – 800 °C

The XRD diagrams of powder materials of samples S_400 and S_800, doped with Zn, are presented in Fig. 3. The powder material, doped with Zn and sintered at 400 °C, is composed of brookite phase of TiO_2 and simonkolleite $Zn_5(OH)_8Cl_2.(H_2O)$ (Fig. 3, a). The presence of Cl-containing derivative compounds can be explained by considering that hydrochloric acid was used for acidification of the initial sol-gel system.

The XRD analysis of the powder material doped with Zn and sintered at 800 °C shows that phase transition of TiO_2 to rutile phase proceeds, concordantly with formation of ecandrewsite $ZnTiO_3$ phase (Fig. 3, b).

The structural differences, combined with the formation of Zn-Ti-O compounds, determine the different electrical characteristics of the Zn-doped humidity sensing elements.

3.2. Electrical measurements

Electrical measurements were taken in alternating current in order to avoid polarization effects in samples in direct current, related to the presence of ionic conduction along with electron conduction in metal oxide humidity sensor elements [7, 15], to which the studied samples refer. The elements are normally represented by equivalent circuits, containing resistors and capacitors [41, 42].

Fig. 4 and Fig. 5 present the characteristics $R = f(RH)$ and $C = f(RH)$ of samples S_400 and S_800, at different frequencies in the range from 100 Hz to 10 kHz and at a temperature of 25 °C.

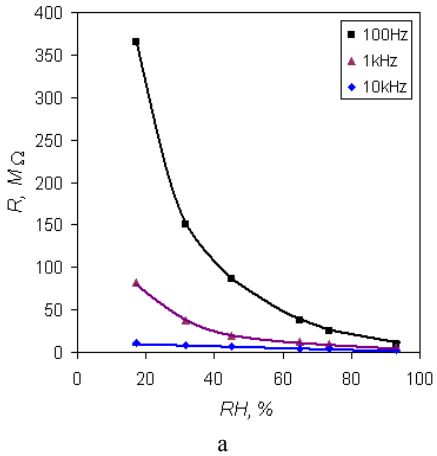

a

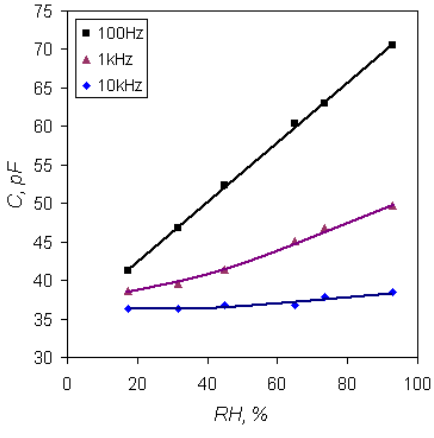

b

Fig. 4. Characteristics of sample S_400 at 25 °C: a – $R = f(RH)$; b – $C = f(RH)$

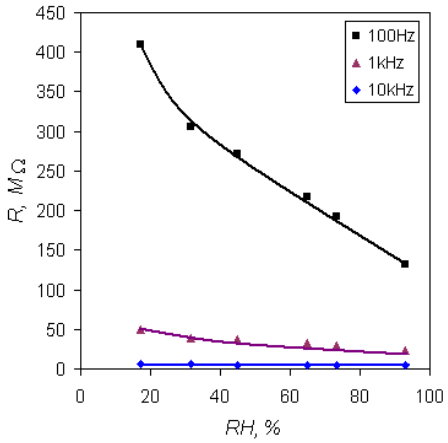

a

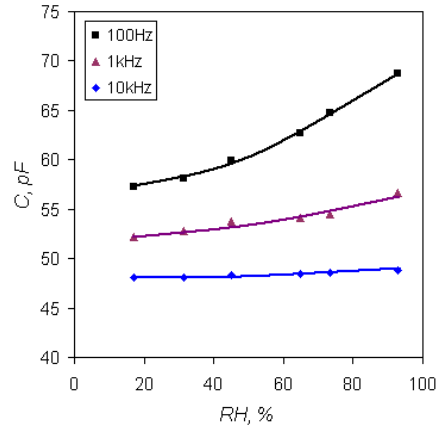

b

Fig. 5. Characteristics of sample S_800 at 25 °C: a – $R = f(RH)$; b – $C = f(RH)$

The investigated humidity sensing elements, as other metal oxide humidity sensors, typically have high electrical resistance at low humidity levels. Therefore, the decrease in this resistance as frequency increases, as shown in Fig. 4 and Fig. 5, is favorable for the implementation of these sensor elements in electric circuits for automatic measurement and control. Nevertheless, as the frequency rises, the variation range of both parameters R and C substantially decreases over 1 kHz, which would restrict their use as humidity sensing elements at higher frequencies, as can be seen in Fig. 4 and Fig. 5. Because of this the results obtained for frequencies 100 kHz and 1 MHz are not presented in these figures. Moreover, electrical resistance R has greater relative change R_{max}/R_{min} in the range from 15 % to 93 %RH compared to the relative change C_{max}/C_{min} in capacitance C and therefore, the parameter R is more informative than C.

Water adsorption and condensation lead to a decrease of the resistance of the investigated samples with an increase in the relative humidity [7]. For the specific segments of characteristics $R = f(RH\,\%)$ of sensor elements, sensitivity S_R is determined by:

$$S_R = \left|\Delta R / \Delta RH\right| , \quad (1)$$

where ΔR is the change in resistance, and ΔRH is the change in relative humidity for the respective segment.

Sample S_400, sintered at 400 °C, has the highest sensitivity, which at 100 Hz reaches 15.1 MΩ/%RH at low ranges of the relative humidity. The sensitivity of the same sample at a frequency of 1 kHz is lower and it reaches 3.2 MΩ/%RH.

Sample S_800, sintered at 800 °C, has a lower sensitivity S_R, compared to sample S_400 and at 100 Hz the maximal value of S_R is 6.4 MΩ/%RH. At a frequency of 1 kHz this sensitivity is 698.6 kΩ/%RH.

The characteristics $R = f(RH)$ of samples S_400, S_800 are compared with those of the referent ones SRef_400, SRef_800 at 100 Hz and 25 °C. The comparison among these characteristics, represented in Fig. 6, enables the assessment of the contribution of the Zn-dopant to the properties of the sensor elements.

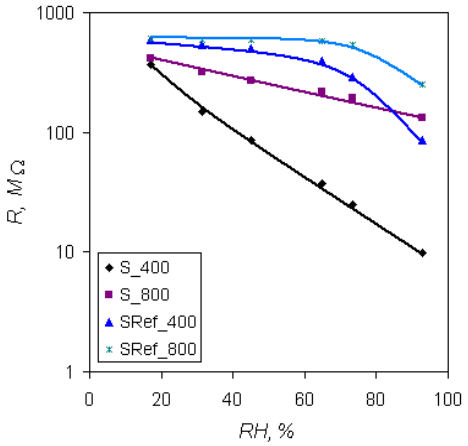

Fig. 6. Characteristics $R = f(RH)$ of samples S_400, S_800, SRef_400 and SRef_800 at 100 Hz and 25 °C

The comparison of the characteristics shown in Fig. 6 reveals that the addition of Zn results in improvement of the sensitivity of both samples S_400 and S_800 for the entire RH range between 15 %RH and 93 %RH, whereas in the referent samples sensitivity increases only for RH levels above 65 % in SRef_400 and 73 % in SRef_800, respectively. After sintering at 800 °C, the referent samples have a narrower range of variation of the resistance, compared to that of the Zn-doped ones. Referent samples have switch-type characteristics and their sensitivity sharply rises at high humidity levels (up to nearly 10.4 MΩ/%RH for SRef_400 and 9.3 MΩ/%RH for SRef_800, respectively).

Consequently, the investigated Zn-containing samples have better humidity sensing properties in the entire range between 15 %RH and 93 %RH than the undoped referent samples. Additionally, their characteristics are practically linear in semi-logharithmic plots, enabling their integration into measuring circuits with logarithmic signal converting elements. Sample S_400 exhibits the highest sensitivity, and its electric resistance changes about 40 fold at 100 Hz for the entire RH range.

During the initial stage of adsorption, there is chemical adsorption of water molecules on the surface of the respective sensors. After the formation of the first chemically adsorbed film there is physical adsorption of water molecules on it, resulting in aggregation of water molecules [7, 16]. The chemical adsorption is related to the prevailing type of electron conduction, whereas the physical adsorption predetermines the predominance of ionic type conduction [41, 42].

The samples sintered at 400 °C have higher sensitivity, compared to these, prepared at 800 °C, because of the beneficial effect of the simonkolleite phase, owing to its remarkable hygroscopicity. Simonkolleite stays at equilibrium with the water content in the air [43, 44]. The presence of brookite phase also contributes to water adsorption [45], promoting supplemental rise of the sensitivity of S_400. For this sensor, remarkable sensitivity was registered at low humidity levels, due to the good chemical adsorption.

Regarding the samples sintered at 800 °C, the extended sensitivity of the Zn containing samples compared to the undoped ones, can be explained by the presence of ecandrewsite $ZnTiO_3$ phase, which is more hygroscopic [30], compared to the rutile phase in the referent samples sintered at 800 °C without dopants. Regardless of the superior porosity of samples S_800, in comparison to this of S_400, the rate of chemical adsorption due to the simonkolleite and brookite phases results in the stronger decrease of the electrical resistance of samples S_400 at lower humidity levels. In the case of S_800, the chemical adsorption is lower and causes a slower decrease of the electrical resistance and with the increase of the relative humidity gradually increases physical adsorption.

As the physical adsorbed layers of water molecules increase, there is a gradual process of capillary condensation of water vapors according to Kelvin's equation [16, 31, 46], resulting also in a decrease of the electrical resistance as relative humidity elevates.

The hysteresis of the characteristics of the studied humidity elements is determined by measuring the resistance of the samples as relative humidity rises from 15 % to 93 %, and then – in reverse direction. The hysteresis of the characteristics $R = f(RH\ \%)$ is determined by:

$$F = (\Delta R_{max} / R_{FS}) \times 100\ \%, \qquad (2)$$

where ΔR_{max} is the maximal difference in sample resistance between the samples characteristics under humidity adsorption and desorption, and R_{FS} is the variation range of resistance.

Fig. 7 shows the characteristics of sample S_400 for humidity adsorption and desorption at a frequency of 100 Hz and 25 °C. On their basis the hysteresis F of the sample has been determined, which is 3.4 %. For sample S_800 hysteresis F is about 2.8 %.

Fig. 8 presents the response characteristics for adsorption and desorption of sample S_400 at a frequency of 100 Hz and 25 °C. The response time for adsorption and desorption is defined as the time taken to reach a value of:

$$(R_{B2} + 10\% R_{FS}) \text{ and } (R_{B1} - 10\% R_{FS}), \qquad (3)$$

respectively, where R_{B1} and R_{B2} are the resistance values at the respective low and high base humidity levels, and R_{FS} is the variation range of resistance between these levels. The base relative humidity levels used are RH_{B1} = 15 % and RH_{B2} = 93 %.

The response times for adsorption and desorption of sample S_400 at a frequency of 100 Hz and 25 °C are respectively: t_{ads} = 65 s, t_{des} =310 s. The obtained response time for adsorption and desorption for sample S_800 at a frequency of 100 Hz and 25 °C are smaller t_{ads} = 56 s, t_{des} = 294 s.

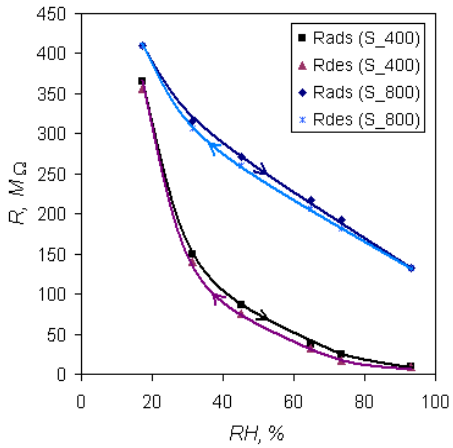

Fig. 7. Hysteresis of samples S_400 and S_800 at 100 Hz and 25 °C: Rads and Rdes – resistance at adsorption and desorption

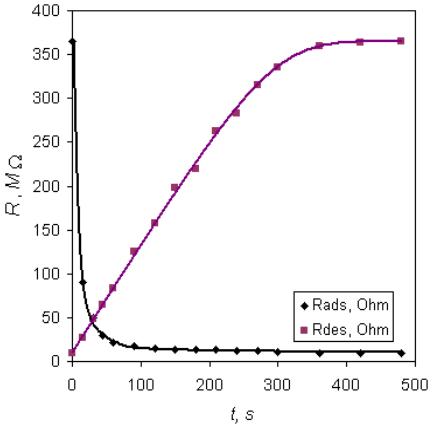

Fig. 8. Response characteristics of the sample S_400 at 100 Hz and 25 °C

Five samples of each type S_400 and S_800 have been examined. After a statistical analysis of the results obtained it has been determined that the deviation of the parameters obtained is within ±5 %, which characterizes their reproducibility.

The variation of the characteristics of the corresponding sensor elements did not exceed 6 % in the course of one year, revealing their stability.

On the basis of the obtained characteristics it can be concluded that both types of samples S_400 and S_800 can be used as humidity sensing elements changing their resistance. Sample S_400 has better properties when humidity changes. Owing to the great decrease in their sensitivity when frequency increases, it is appropriate to be connected to measuring circuits at frequencies of up to 1 kHz.

The values of the parameters of the investigated humidity sensors are comparable to those of the bulk ceramic and nano-structured sensor elements, composed of TiO_2-ZnO. However the relative change R_{max}/R_{min} of the resistance for S_400 at 100 Hz in the range from 15 %RH to 93 %RH is around 40 and is higher than this one of other samples based on a TiO_2-ZnO system, where R_{max}/R_{min} varies from about 3 to 20. Another advantage of the studied sensors is the relative simplicity of the method of their preparation, which requires inexpensive precursors and equipment.

4. CONCLUSIONS

The use of the sol-gel method enables the synthesis of thin film humidity sensor elements based on Zn doped TiO_2. These sensors can be used for the entire humidity range from 15 %RH to 93 %RH. This method is easily applicable to the investigated TiO_2-ZnO system and requires inexpensive precursors and equipment. The Zn-dopant increases the sensitivity of the respective sensors and the measurement humidity range.

The sensitivity of samples S_400 at low humidity levels measured at frequency from 100 Hz and 25 °C is of the order of 15.1 MΩ/%RH, whereas for samples S_800 it is 6.4 MΩ/%RH. In comparison with other samples based on a TiO_2-ZnO system, the relative change R_{max}/R_{min} of the resistance for S_400 at 100 Hz in the range from 15 %RH to 93 %RH is higher and is around 40. The hysteresis of the samples S_400 and S_800 is of the order of 3.4 % – 2.8 %, response time for adsorption is 65 s – 56 s, and for desorption – around 310 s – 294 s, respectively. Increasing the frequency decreases the resistance of the samples at low humidity but also decreases their sensitivity. Therefore, they are appropriate for use at frequencies of up to 1 kHz. The characteristics of S_400 and S_800 in semi-logarithmic plot are practically linear, enabling their integration in logarithmic measuring circuits. Therefore, both types of obtained samples, S_400 and S_800, can be used successfully as humidity sensing elements at lower frequencies. Sample S_400 has the highest sensitivity properties among the investigated sensors mainly due to the presence of simonkolleite phase that possesses good chemical adsorption capability.

Acknowledgments

This work was supported by the National Scientific Research Fund of Bulgaria under Contract № DO 02-148/2008.

REFERENCES

1. **Rittersma, Z. M.** Recent Achievements in Miniaturized Humidity Sensors – a Review of Transduction Techniques *Sensors and Actuators A* 96 2002: pp. 196 – 210.
2. **Lee, C. Y., Lee, G. B.** Humidity Sensors: A Review *Sensor Letters* 3 2005: pp. 1 – 15.
3. **Sakai, Y., Sadaoka, M.** Humidity Sensors Based on Polymer Thin Films *Sensors and Actuators B* 35 – 36 1996: pp. 85 – 90.
4. **Sakai, Y., Matsuguchi, M.; Hurukawa, T.,** Humidity Sensor Using Crosslinked Poly(chloromethyl Styrene) *Sensors and Actuators B* 66 2000: pp. 135 – 138.
5. **Su, P. G., Sun, Y. L., Lin, C. C.** Humidity Sensor Based on PMMA Simultaneously Doped with Two Different Salts *Sensors and Actuators B* 113 2006: pp. 883 – 886.
6. **Wang, J., Shi, K.** Study of Polymer Humidity Sensor Array on Silicon Wafer *Journal of Materials Science* 39 2004: pp. 3155 – 3157.
7. **Seiyama, T., Yamazoe, N., Arai, H.** Ceramic Humidity Sensors *Sensors and Actuators* 4 1983: pp. 85 – 96.
8. **Nenov, T. G., Yordanov, S. P.** Ceramic Sensor Device Materials *Sensors and Actuators B* 8 1992: pp. 117 – 122.
9. **Tai, W.-P., Oh, J.-H.** Fabrication and Humidity Sensing Properties of Nanostructured TiO_2-SnO_2 Thin Films *Sensors and Actuators B* 85 2002: pp. 154 – 157.
10. **Qi, Q., Feng, Y., Zhang, T., Zheng, X., Lu, G.** Influence of Crystallographic Structure on the Humidity Sensing Properties of KCl-Doped TiO_2 Nanofibers *Sensors and Actuators B* 139 2009: pp. 611 – 617.
11. **Li, Y., Yang, M. J., She, Y.** Humidity Sensors Using in situ Synthesized Sodium Polystyrenesulfonate/ZnO Nanocomposites *Talanta* 62 2004: pp. 707 – 712.
12. **Patil, D., Seo, Y.-K., Hwang, Y. K., Chang, J.-S., Patil, P.** Humidity Sensitive Poly(2,5-dimethoxyaniline)/WO_3 Composites *Sensors and Actuators B* 132 2008: pp. 116 – 124.
13. **Parvatika, N., Jain, S., Khasim, S., Revansiddappa, M., Bhoraskar, S. V., Ambika Prasad, M. V. N.** Electrical and Humidity Sensing Properties of Polyaniline/WO_3 Composites *Sensors and Actuators B* 114 2006: pp. 599 – 603.
14. **Su, P.-G., Hung, L.-N.** Humidity Sensors Based on TiO_2 Nanoparticles/polypyrrole Composite Thin Films *Sensors and Actuators B* 123 2007: pp. 501 – 507.
15. **Nenov, T., Yordanov, S.** Ceramic Sensors: Technology and Applications. Technomic Publ. Co. Inc.: Lancaster, USA, 1996: pp. 10 – 14.
16. **Traversa, E.** Ceramic Sensors for Humidity Detection: The State-of-The-Art and Future Developments *Sensors and Actuators B* 23 1995: pp. 135 – 156.
17. **Katayama, K., Hasegawa, K., Takanashi, Y., Akira, T.** Humidity Sensitivity of Nb_2O_5-Doped TiO_2 Ceramics *Sensors and Actuators A* 24 1990: pp. 55 – 60.
18. **Yeh, Y. C., Tseng, T. Y., Chang, D. A.** Electrical Properties of TiO_2-$K_2Ti_{16}O_{13}$ Porous Ceramic Humidity Sensor *Journal of the American Ceramic Society* 73 (7) 1990: pp. 1992 – 1998.
19. **Tai, W.-P., Oh, J.-H.** Fabrication and Humidity Sensing Properties of Nanostructured TiO_2-SnO_2 Thin Films *Sensors and Actuators B* 85 2002: pp. 154 – 157.
20. **Aoki, H., Azuma, Y., Asaka, T., Higuchi, M., Asaga, K., Katayama, K.** Improvement of Response Characteristics of TiO_2 Humidity Sensors by Simultaneous Addition of Li_2O and V_2O_5 *Ceramics International* 34 2008: pp. 819 – 822.
21. **Faia, P. M., Ferreira, A. J., Furtado, C. S.** Establishing and Interpreting an Electrical Circuit Representing a TiO_2-WO_3 Series of Humidity Thick Film Sensors *Sensors and Actuators B* 140 2009: pp. 28 – 133.
22. **Qi, Q., Zhang, T., Yu, Q., Wang, R., Zeng, Y., Liu, L., Yang, H.** Properties of Humidity Sensing ZnO Nanorods-Base Sensor Fabricated by Screen-Printing *Sensors and Actuators B* 133 2008: pp. 638 – 643.
23. **Yadav, B. C., Srivastava, R., Dwivedi, C. D., Pramanik, P.** Moisture Sensor Based on ZnO Nanomaterial Synthesized through Oxalate Route *Sensors and Actuators B* 131 2008: pp. 216 – 222.
24. **Srivastava, R., Yadav, B. C., Dwivedi, C. D., Kumar, R.** Comparative Study of Moisture Sensing Properties of ZnO Nanomaterials through Hydroxide Route by Mixing Dropwise and Sudden *Sensors and Transducers Journal* 80 (6) 2007: pp. 1295 – 1301.
25. **Qi, Q., Zhang, T., Zeng, Y., Yang, H.** Humidity Sensing Properties of KCl-doped Cu–Zn/CuO–ZnO Nanoparticles *Sensors and Actuators B* 137 2009: pp. 21 – 26.
26. **Qi, Q., Zhang, T., Wang, S., Zheng, X.** Humidity Sensing Properties of KCl-Doped ZnO Nanofibers with Super-Rapid

Response and Recovery *Sensors and Actuators B* 137 2009: pp. 649 – 655.

27. **Joanni, E., Baptista, J. L.** ZnO-Li_2O Humidity Sensors *Sensors and Actuators B* 17 1993: pp. 69 – 75.
28. **Mineiro, S.L., Nono, M. C. A., Kuranaga, C., Silva, M. D.** Humidity Sensitive Characteristics of ZnO-TiO_2-Ta_2O_5 Ceramic *Materials Science Forum* 498 – 499 2005: pp. 293 – 298.
29. **Wang, W., Li, Z., Liu, L., Zhang, H., Zheng, W., Wang, Y., Huang, H., Wang, Z., Wang, C.** Humidity Sensor Based on LiCl-Doped ZnO Electrospun Nanofibers *Sensors and Actuators B* 141 2009: pp. 404 – 409.
30. **Pandey, N. K., Tiwari, K., Akash, R.,** ZnO-TiO_2 Nanocomposite: Characterization and Moisture Sensing Studies *Bulletin of Materials Science* 35 (3) 2012: pp. 347 – 352.
31. **Srivastava, R., Yadav, B. C.** Nanaostructured ZnO, ZnO-TiO_2 and ZnO-Nb_2O_5 as Solid State Humidity Sensor *Advanced Materials Letters* 3 (3) 2012: pp. 197 – 203.
32. **Jagtap, Sh., Priolkar, K. R.** Evaluation of ZnO Nanoparticles and Study of ZnO-TiO_2 Composites for Lead Free Humidity Sensors *Sensors and Actuators B* 183 (5) 2013: pp. 411 – 418.
33. **Faia, P. M., Furtado, C. S.** Effect of Composition on Electrical Response to Humidity of TiO_2:ZnO Sensors Investigated by Impedance Spectroscopy *Sensors and Actuators B* 181 2013:pp. 720 – 729.
34. EU Directive 2002/95/EC. Restriction of Hazardous Substances in Electrical and Electronic Equipment (RoHS directive 2002). Available online: http://ec.europa.eu/environment/waste/rohs_eee/legis_en.htm.
35. U.S. Department of Health and Human Services; Public Health Service; Agency for Toxic Substances and Disease Registry. Toxicological profile for Chromium, 2012. Available online: http://www.atsdr.cdc.gov/toxprofiles/tp7.pdf .
36. **Das, P., Butcher, R. J., Mukhopadhyay, C.** Zinc Titanate Nanopowder: an Advanced Nanotechnology Based Recyclable Heterogeneous Catalyst for The One-Pot Selective Synthesis of Self-Aggregated Low-Molecular Mass Acceptor-Donor-Acceptor-Acceptor Systems and Acceptor-Donor-Acceptor Triads *Green Chemistry* 14 2012: pp. 1376 – 1387.
37. **Chang, Y.-S., Chang, Y.-H., Chen, I.-G., Chen, G.-J., Chai, Y.-L., Fang, T.-H., Wu, S.** Synthesis, Formation and Characterization of $ZnTiO_3$ Ceramics *Ceramics International* 30 2004: pp. 2183 – 2189.
38. JCPDS Crystal Data Determinative Tables, Inorganic compounds, 3-rd Edition. **H. Ondik, A. Mighell**, Eds.; US NSRDS Publ.: USA, Volume 4, 1978: p.17.
39. **Linsebigler, A., Lu, G., Yate, J.** Photocatalysis on TiO_2 Surfaces: Principles, Mechanisms, and Selected Results *Chemical Reviews* 95 1995: pp. 735 – 758.
40. **Dorian, A. H., Sorrell, C. C.** Review of the Anatase to Rutile Phase Transformation *Journal of Materials Science* 46 (4) 2011: pp. 855 – 874.
41. **Dickey, E. C., Varghese, O. K., Ong, K. G., Gong, D. W., Paulose, M., Grimes, C. A.** Room Temperature Ammonia and Humidity Sensing Using Highly Ordered Nanoporous Alumina Films *Sensors* 2 2002: pp. 91 – 110.
42. **Zhang, Yi., Chen, Y., Zhang, Yu., Cheng, X., Feng, C., Chen, L., Zhou□,J., Ruan, S.** A Novel Humidity Sensor Based on $NaTaO_3$ Nanocrystalline *Sensors and Actuators B* 174 2012: pp. 485 – 489.
43. **Garcia-Martinez, O., Vila, E., Martin de Vidales, J. L., Rojas, R. M., Petrov, K.** On the Thermal Decomposition of the Zinc(II) Hydroxide Chlorides $Zn_5(OH)_8Cl_2{\cdot}(H_2O)$ and Beta-Zn(OH)Cl *Journal of Materials Science* 29 1994: pp. 5429 – 5434.
44. **Rasines, I., Morales, J. I.** Thermal Analysis of Beta-$Co_2(OH)_3Cl$ and $Zn_5(OH)_8Cl_2{\cdot}(H_2O)$ *Thermochimica Acta* 37 1980: pp. 239 – 246.
45. **Chen, Z., Lu, C.** Humidity Sensors: A Review of Materials and Mechanisms *Sensor Letters* 3 2005: pp. 274 – 295.
46. **Shimizu, Y., Arai, H., Seiyama, T.** Theoretical Studies on the Impedance Humidity Characteristics of Ceramic Humidity Sensors *Sensors and Actuators B* 7 1985: pp. 11 – 22.